Journal of Hydrology 617 (2023) 128925

Contents lists available at ScienceDirect

Journal of Hydrology

journal homepage: www.elsevier.com/locate/jhydrol

Research papers

Modeling the spatial distribution of the meteoric water line of modern precipitation across the broader Mediterranean region

István Gábor Hatvani [a,b], Alaa Eddine Smati [c], Dániel Erdélyi [c,d], Gábor Szatmári [e,f], Polona Vreča [g], Zoltán Kern [a,b,*]

[a] Institute for Geological and Geochemical Research, Research Centre for Astronomy and Earth Sciences, Budaörsi út 45, H-1112 Budapest, Hungary
[b] CSFK, MTA Centre of Excellence, Budapest, Konkoly Thege Miklós út 15-17, 1121 Budapest, Hungary
[c] Department of Geology, Eötvös Loránd University, Pázmány Péter stny. 1, H-1117 Budapest, Hungary
[d] Doctoral School of Environmental Sciences, Eötvös Loránd University, Pázmány Péter stny 1, H-1117 Budapest, Hungary
[e] Institute for Soil Sciences, Centre for Agricultural Research, Herman Ottó út 15, H-1022 Budapest, Hungary
[f] Department of Physical Geography and Geoinformatics, University of Debrecen, Egyetem tér 1, H-4032 Debrecen, Hungary
[g] Department of Environmental Sciences, Jožef Stefan Institute, Jamova Cesta 39, 1000 Ljubljana, Slovenia

ARTICLE INFO

This manuscript was handled by Marco Borga, Editor-in-Chief.

Keywords:
Meteoric water line
Stable isotopes
RMA regression
Machine learning
Precipitation
EMMWL
WMMWL

ABSTRACT

The covariance of stable hydrogen (δ^2H) and oxygen (δ^{18}O) isotopes in local precipitation (the local meteoric water line – LMWL) serves as a benchmark in isotope hydrological or paleoclimatological applications. However, the isotope hydrometeorological monitoring network is still sparse in many parts of the Mediterranean, and the degree of spatial data coverage is insufficient to address current needs. To remedy this weakness a spatially continuous interpolated geostatistical product of the LMWLs of modern precipitation across the Mediterranean has been developed. The LMWLs of the stations with data for more than four years between 2000 and 2015 were calculated using reduced major axis regression, and then interpolated across the region using statistical and machine learning methods. Random forest interpolation with buffer distance and elevation gave the best performance in the out-of-sample verification, and was thus used to derive the final interpolated product. The slope and intercept of the LMWLs ranged between ~5.9 to 8.2 and −3.9 to 16.1‰, respectively. A detailed comparison with previous local/regional estimations showed that the model presented here concurs with those, albeit with minor deviations in certain regions. With the present results, it then becomes possible to assess how well grounded the 'Eastern- and Western Mediterranean Meteoric Water Lines' (EMMWL and WMMWL) for the 21st century are. In the eastern Mediterranean, the current model shows a slope (~6.9) and the intercept (~15‰) concurring with local studies, but does not reproduce the frequently cited benchmark values of the EMMWL; slope: 8, intercept ≥20‰. The EMMWL may be considered an idealized isotope-hydrological benchmark useful in regional studies; nonetheless, it cannot be taken as a valid representation of the actual empirical description of the δ^2H – δ^{18}O covariance of local precipitation in the eastern Mediterranean. Defining a uniform regional MWL in the western Mediterranean is not supported by the spatial heterogeneity of LMWL parameters based on the present estimations, calling into question the utility of the 'WMMWL' as an isotope hydrological benchmark.

1. Introduction

Water phase changes occur over various spatiotemporal scales in the global hydrological cycle, resulting in relative changes in the spatiotemporal distribution of stable water isotopes (Yoshimura, 2015). The specific isotopic signatures of atmospheric processes such as evaporation, condensation, and deposition in precipitation are then imprinted in terrestrial water bodies, allowing the application of isotopic data to hydrological studies (Gat et al., 2001). The isotopic composition of hydrogen (δ^2H) and oxygen (δ^{18}O) of precipitation (δ_p) is recognized as highly important natural tracer in the water cycle (Bowen et al., 2019; Fórizs, 2003; Gat, 1996; Gat et al., 2001).

Abbreviations: RMA, Reduced major axis; EMMWL, Eastern Mediterranean Meteoric Water Line; WMMWL, Western Mediterranean Meteoric Water Line.

* Corresponding author at: Institute for Geological and Geochemical Research, Research Centre for Astronomy and Earth Sciences, Budaörsi út 45, H-1112 Budapest, Hungary.
E-mail addresses: szatmari@rissac.hu (G. Szatmári), polona.vreca@ijs.si (P. Vreča), kern.zoltan@csfk.org, zoltan.kern@gmail.com (Z. Kern).

https://doi.org/10.1016/j.jhydrol.2022.128925
Received 6 April 2022; Received in revised form 2 December 2022; Accepted 3 December 2022
Available online 15 December 2022

Describing the linear relationship between δ^2H and $\delta^{18}O$ in precipitation is a classical concept of hydrology (Gat, 2005), and is called the meteoric water line (MWL). It is common practice to define a 'Local Meteoric Water Line' (LMWL) for a given location as the best linear fit of all the precipitation data in δ-space (Gat, 2005). A global compilation of the δ^2H and $\delta^{18}O$ of fresh water provided a best-fit line, $\delta^2H = 8 \times \delta^{18}O + 10$ (Craig, 1961), later called the Global Meteoric Water Line (GMWL). Following an additional ~30-years of data collection, the database of Global Network of Isotopes in Precipitation (GNIP) allowed the GMWL's revision based on long-term amount-weighted annual means as $\delta^2H = 8.20\ (\pm 0.07) \times \delta^{18}O + 11.27\ (\pm 0.65)$ (Rozanski et al., 1993).

The GMWL is very useful in hydrology in understanding the origin of modern and ancient ground water and its interactions with surface waters. The GMWL may be considered an amalgamation of many local meteoric water lines (LMWL) which, in turn, vary greatly in their slope and intercepts on regional or local scales (Kendall and Coplen, 2001; Sharp, 2017). These LMWLs are often evaluated in the context of their deviation from the GMWL – e.g. Tappa et al. (2016)-, which represents the "expected" equilibrium relationship, where the slope is assumed to arise from the ratio of equilibrium fractionation factors (Putman et al., 2019).

The GMWL's slope of 8 reflects the average global relationship between δ^2H and $\delta^{18}O$ in precipitation, while LMWL slopes documented at values ranging from 4.8 to 10.9 at ~400 sites globally (Putman et al., 2019) may indicate that at least one season is characterized by precipitation affected by nonequilibrium processes. The intercept of the LMWLs has also been documented as varying across the globe from −24‰ to +27‰ (Putman et al., 2019).

The LMWL represents the characteristic distribution of δ_p and can, if determined from long-term observations, serve as a benchmark in isotope hydrological applications such as the estimation of the infiltration period, or the paleoclimatological evaluation of the groundwater isotope signals (Clark and Fritz, 1997). It is common practice, however, to estimate the LMWLs from just short-term investigations – e.g. Bottyán et al. (2017); El Ouali et al. (2022); Kattan (1997); Liotta et al. (2013); Paar et al. (2019) – an approach which is prone to biasing by anomalous climatic events (Longinelli et al., 2006; Vreča et al., 2007; Vreča et al., 2022). If at least 48 months' data for a given station is used, it can attenuate the possible noise caused by such extreme events and interannual variability in estimating the covariance of δ^2H and $\delta^{18}O$ (Putman et al., 2019).

At present the Mediterranean region faces an ever-increasing tendency towards water shortage (García-Ruiz et al., 2011; Hoerling et al., 2012; Iglesias et al., 2007; Villani et al., 2022), which will clearly amplify the potential for sociopolitical and economic disruption, e.g., Kelley et al. (2015), and ecological problems (Cook et al., 2016). Isotope hydrological methods have great potential in the improvement of the scientific understanding of the processes governing the regional water cycle, and so, therefore, to assist in knowledge-based water-resource management (Aggarwal et al., 2005). In some parts of the Mediterranean region the isotope hydrometeorological monitoring network was sparse in the past, leading to the initiation of regional campaigns (IAEA, 2005) and further subregional monitoring. The spatial data coverage is, however, still insufficient for many scientific purposes.

Isotope hydrological studies frequently use LMWLs across the Mediterranean, tackling problems in subsurface (Brkić et al., 2020; Christofi et al., 2020; Hssaisoune et al., 2022; Koeniger et al., 2017; Liotta et al., 2013; Trabelsi et al., 2020; Túri et al., 2020; Vasić et al., 2019) or surface hydrology (El Ouali et al., 2022; Gat and Dansgaard, 1972; Serianz et al., 2021). LMWLs taken from relatively remote locations have recently started to grow in numbers, e.g., Boumaiza et al. (2021); Elghawi et al. (2021); Túri (2019), indicating a great demand for such reference data in the isotope hydrological research in the region. Therefore, reliable estimates of the LMWLs are also important at places where direct isotope meteorological monitoring is not in operation. Remote LMWLs can indeed be misleading for local water resource applications, e.g. Serianz et al. (2021).

The LMWLs might be very similar over extended regions, allowing the definition of regional MWLs. Pioneering studies have assessed the precipitation stable isotope composition on subregional scales in the broader Mediterranean realm. Regional meteoric water lines for the eastern- (EMMWL; $\delta^2H = 8 \times \delta^{18}O + 22$), and the western parts (WMMWL; $\delta^2H = 8 \times \delta^{18}O + 13.7$) were established in the late 20th century and both continue to serve as widely used benchmarks in isotope hydrological studies (Fernández-Chacón et al., 2010; Giustini et al., 2016; Natali et al., 2021; Surić et al., 2018).

Previously determined models can require revision because of the ongoing spatiotemporally varying changes in the hydroclimate, which may be presumed to induce alterations in the isotope-hydrometeorological signal. A further source of difficulty is the existence of various methodological approaches to addressing the question of describing the linear relationship between the water stable isotopes across the Mediterranean (e.g. Argiriou and Lykoudis (2006)), and these may be expected to result in significantly different estimates (Crawford et al., 2014; Marchina et al., 2020; Natali et al., 2021). Moreover, the temporal resolution of the input data and most importantly, the time period the data cover can cause significant differences in the estimates of the slope and intercept of the LMWLs (Putman et al., 2019), as has been specifically documented in certain sub-regions of the Mediterranean; e.g. Krajcar Bronić et al. (2020a); Vreča and Malenšek (2016).

The regional MWL was defined in the western Mediterranean (WMMWL) on the basis of data from ten coastal stations with relatively short-term coverage from the end of the twentieth century (Celle-Jeanton et al., 2001). The origin of the Eastern Mediterranean meteoric water line (EMMWL) is somehow more obscure. In the eastern Mediterranean it was found that the d excess, a second-order stable isotopic parameter (defined as $d = \delta^2H - 8 \times \delta^{18}O$ (Dansgaard, 1964)) has characteristically elevated values (well above 18‰) (Gat and Carmi, 1970). This observation for Eastern Mediterranean precipitation subsequently received reinforcement: $d >$ 15‰ (El-Asrag, 2005; Rindsberger et al., 1990). To complicate the issue further, decades later, in Gat (1996) this same observation was referred to as "… the eastern Mediterranean–MWL of $d \sim$ 20‰ Gat and Carmi (1970)…".

Regarding the slope of an eastern Mediterranean regional meteoric water line there is no mention of it in Gat and Carmi (1970). A relationship between precipitation δ^2H and $\delta^{18}O$ samples has been documented for Israel with slopes of 5 and 6.3 (Gat and Dansgaard (1972): Fig. 3 therein). A potential source of misunderstanding could be the first numeric appearance of the 'rather well known' equation: $\delta^2H = 8 \times \delta^{18}O + 22$ in relation with isotope data of surface water in the Upper Jordan Valley (Fig. 9 in Gat and Dansgaard (1972)); this, however, clearly cannot be taken as a figure for precipitation representative of the eastern Mediterranean. Furthermore, Rindsberger et al. (1990) in Sect. 1 states "The δD and $\delta^{18}O$ values of the precipitation, in most cases, follow a relationship such as $\delta D = 8 \times \delta^{18}O + d$, the so-called … MWL relationship", which is clearly an oversimplification of the matter. Meanwhile, Fig. 7A (δ^2H vs. $\delta^{18}O$ plot) in Rindsberger et al. (1990) presents a reference line annotated as "MWL, $d >$ 22‰" without any underlying data or citation, suggesting that this is just an arbitrarily chosen benchmark in that particular study. At the turn of the twenty-first century, it was reported that rain events of > 20 mm at a monitoring station in Israel between 1995 and 1997, followed a "trend with a slope of ~8, and d-excess of 20 to 30‰" (Ayalon et al., 1998). This, however, cannot be considered an MWL, since as noted above, the LMWL is defined as the best linear fit of all the precipitation data in δ-space (Gat, 2005).

It seems that some studies have taken it for granted that the slope is 8 and the intercept is 22‰ of the EMMWL, although these parameters were not obtained obeying the rules of how meteoric water lines should be derived; see Gat (2005). What is more, further confusion regarding the Mediterranean regional meteoric water lines may have originated from the occasional usage of ad-hoc terminology and acronyms. For example, the Mediterranean Meteoric Water Line (MMWL (Ayalon et al.,

1998; Koeniger et al., 2017)), which is used to represent location(s) in the eastern Mediterranean, or the abbreviation EMWL (e.g. Bajjali and Abu-Jaber (2001); Yüce (2005)). Such usage further increases the possibility of confusion over regional MWLs. In the present work, the abbreviations EMMWL and WMMWL are used exclusively to refer to the regional definitions.

A recent study has addressed the geographic variations in the slope of LMWLs across Europe focusing on the temperate and boreal regions of the continent (Lécuyer et al., 2020); it does not, however, cover the Mediterranean region. Thus, the current work aims to provide a spatial extension of that analysis with respect to the slope of LWMLs. Additionally, the present study represents a methodological extension, because the intercept of the LMWL is also evaluated. Moreover, in doing so, the performance of various interpolation methods (classical statistical and machine learning) with different set of predictors (altogether 14 approaches) is investigated in modeling the spatial distribution of the slope and intercept of the local meteoric water lines across the Mediterranean taking into consideration the climatic and geographic context of the region.

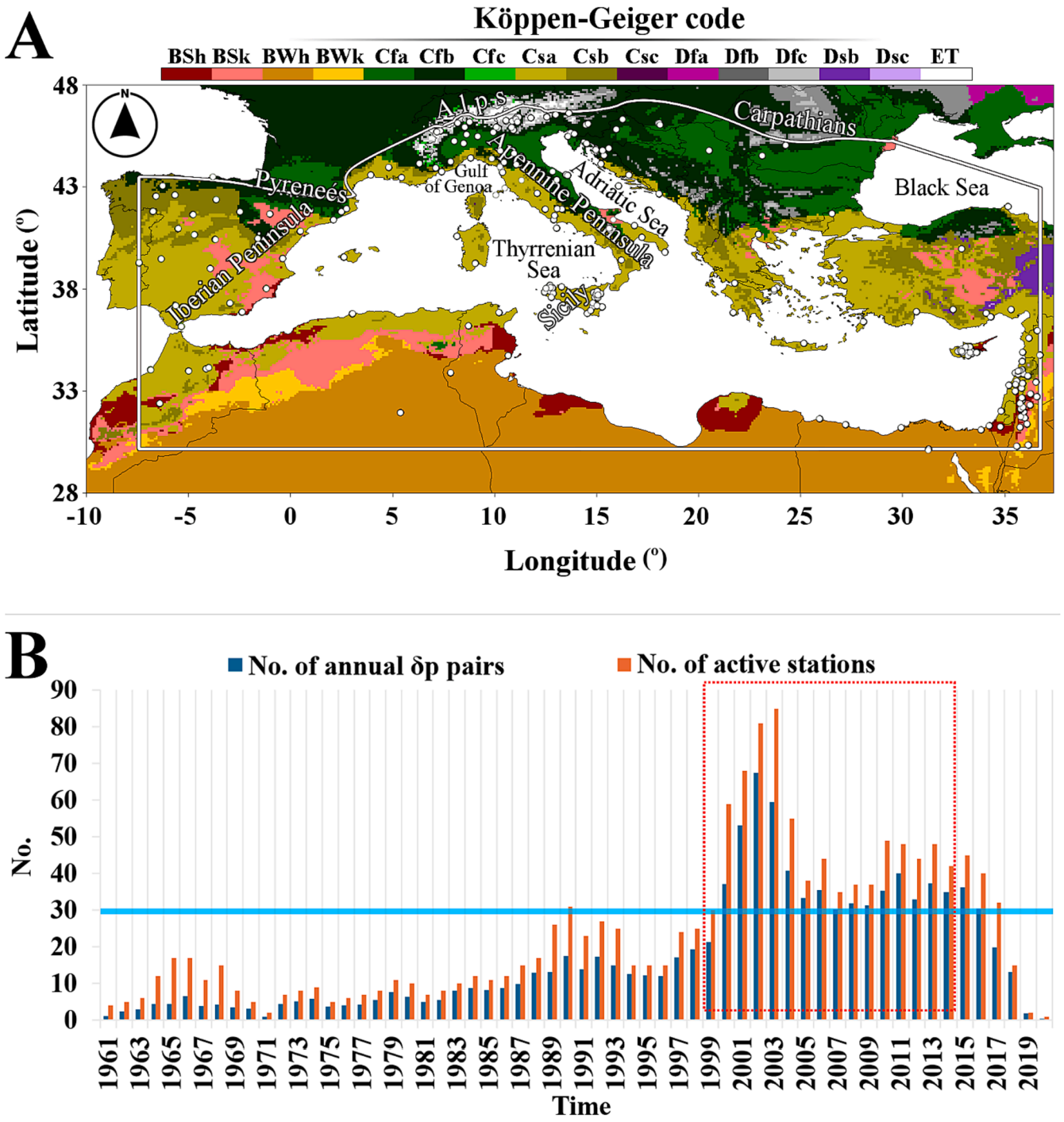

Fig. 1. Study area, monitoring sites and available data. Map of Köppen climate zones (Kottek et al., 2006) and precipitation monitoring sites (white dots) of the region studied (A). Number of δ_p records obtained from the GNIP stations and other data sources (see Sect. 2.2) for the period 1960–2020. The red dotted rectangle represents the focus period for data preprocessing (2000–2015; see Sect. 2.3.1). The horizontal blue line indicates the threshold chosen to select the focus period (B).

2. Materials and methods

2.1. Study area description

The study area covers the Mediterranean Basin from north Africa, across southern Europe to the Middle East. This area extends from 7.5° W to 36.7° E, and from 29.9° N to the orogenic belt from the Pyrenees through the Southern Alps to the Carpathian chains (Fig. 1A).

The Mediterranean climate of the region is characterized by temperate dry hot summers and humid winters, the Csa climate subtype in the Köppen-Geiger climate classification system (Kottek et al., 2006). Warm dry summers (Csb) are more frequent on the coasts close to the Atlantic Ocean in the West and the Black Sea in the East. The southern part of the basin is dominated by arid hot and cold steppe conditions (BSh, BSk) and arid desert conditions (BWh), especially south of 31° N under the influence of the Sahara. North of 41° N, a temperate climate dominates, without a dry season, and with warm (Cfb) and hot summers (Cfa), especially around the Black and Adriatic Seas.

The Mediterranean Basin is characterized by specific patterns of atmospheric circulation, with dry and cold continental air masses that interact with a marine basin characterized by high evaporation rates and relatively high sea surface temperatures (≈ 20 °C) (IAEA, 2005). Such air-sea interactions are important sites of cyclogenesis in the Mediterranean (Bartholy et al., 2009; Kelemen et al., 2015). Compared to the rest of the European continent, which is dominated by Atlantic moisture, the Mediterranean has a more complex moisture source structure, the primary source region being the Mediterranean Sea itself, at least seasonally (Ciric et al., 2018). Previous subregional isotope hydrometeorological assessments have revealed that the variable physiographic and hydrometeorological factors act differently and result in a remarkable divergence in values of δ_p between the different parts of the Mediterranean Basin (Fischer and Mattey, 2012; Giustini et al., 2016; Hatvani et al., 2020; Hunjak et al., 2013). Consequently, the $\delta^2H - \delta^{18}O$ relationship has also been found to display considerable subregional differences; e.g. Dotsika et al. (2010); Giustini et al. (2016); Vreča et al. (2006).

2.2. Data used

Monthly δ_p values were acquired from a total of 249 monitoring stations (covering 1960–2020), primarily from the Global Network of Isotopes in Precipitation (GNIP), with six stations updated with more recent data: Râmnicu Vâlcea (Varlam et al., 2021), Zagreb (Krajcar Bronić et al., 2020a), Plitvice (Krajcar Bronić et al., 2020b), Ljubljana and Portorož (Vreča et al., 2015; Vreča et al., 2011; Vreča et al., 2008; Vreča et al., 2014; Vreča et al., 2022), and Pisa (Natali et al., 2021) (Table S1). In addition, other local and regional networks were included:

- 11 stations in Sicily operating between February 2002 and March 2003 (Liotta et al., 2006); 6 stations (February 1992 to December 1996) (Longinelli and Selmo, 2003); 8 stations (January 2002 – December 2004) scattered across northern Italy (Longinelli et al., 2006), 3 stations from the Mt. Vulture region (Paternoster et al., 2008), and 7 stations from Tuscany (Natali et al., 2021). In addition, single records from Forni di Sopra (2005–2010) (Cervi et al., 2017) and Riva del Garda from February 2007 to January 2008 (Longinelli et al., 2008);
- data collected at 6 stations in Lebanon between October 2012 and May 2013 (Koeniger and Margane, 2014);
- 6 stations in Hungary operating between January 2005 and November 2017 (Fórizs et al., 2020);
- 3 stations in Croatia operating between May 2012 and September 2013 (Paar et al., 2019) and one station between 2017 and 2019 (Marković et al., 2020);
- Dumbrava (Romania) from April 2012 to July 2015 (Bojar et al., 2017);
- 16 stations in Cyprus (2014–2017) (Christofi et al., 2020);
- 1 station in Serbia (1992–1997 and 2003–2005) (Golobočanin et al., 2007); and
- 2 short time series from Morocco from June 2010 to November 2011 (Wassenburg et al., 2016).

In general, the data gathered were unequally distributed in space (Fig. 1A) and time (Fig. 1B). Until the mid-1980s, the number of active precipitation monitoring stations was limited ($n < 12$). From the mid-1980s onwards their number rose progressively, reaching about 50 by the turn of the millennium. In the early 2000s, owing to a coordinated research project of the IAEA (IAEA, 2005), the network was quite extensive. For instance, in 2002/3 the number of active stations peaked at over 80, while the average number of annual δ_p pairs was ~60 at that time (Fig. 1B). In the 2000s the same number of δ^2H and $\delta^{18}O$ data were generally available, although in certain cases the $\delta^{18}O$ records were more abundant.

To maximize the spatiotemporal coverage of the δ_p values available from the study region, a focus period of 2000–2015 was chosen. This period was characterized by an annual average number of stations > 31 providing data in any given year. The only exception was 2007, in which the average number of active stations was only 30.2 (Fig. 1B). Nevertheless, the focus period chosen (2000–2015) was not cut in half on account of this one year.

2.3. Methodology

2.3.1. Data preprocessing

As a first step, local Moran's I statistics (Moran, 1948) were calculated to investigate the correlations within different spatial units and their surrounding spatial lags (up to 501 km). This was done for each month from January 2000 to December 2015 for both δ_p, using Moran scatterplots (Anselin, 1996), classifying the spatial autocorrelation (Moran Is) of the stations into four types, and enabling an advanced screening for outliers.

If the Moran scatterplot suggested a possible error, the d-excess values ($d-excess = \delta^2H - 8 \times \delta^{18}O$ (Dansgaard, 1964)) were also compared between the neighboring. If the d-excess values of the possible outlier deviated inexplicably from its neighbor(s) (e.g. diff. > 10), the δ_p values were dropped; cf. Erdélyi (2023). This approach is more complex than that employed in previous studies, which used a static d-excess cutoff threshold (Bowen, 2008; Nelson et al., 2021), outside of which δ_p values were excluded without any consideration of the spatial relationship.

As a result of this approach, δ_p values from Patras (Dec 2000), Ciudad Real (Feb 2002), Antalya (Mar 2003) and Murcia (Jan 2004) were dropped, in all cases the d-excess was < −20. In addition, curiously in 2010 the exact same δ_p values were recorded at the Ankara and Antalya stations and it was not possible to trace back the origin of the GNIP database error or decide to which station the values belong. Thus, these were excluded from the analyses.

Next, the monitoring stations were classified into three quality categories (QC) according to the number of data recorded at each one during 2000–2015.

- Stations belonging to QC 1 had to have δ^2H–$\delta^{18}O$ pairs from > 48 months, as this was the amount of data required for any LMWL calculation for it to take on the characteristics of the long-term distribution without bias caused by natural noise (Putman et al., 2019).
- In the study area, in high summer, precipitation may not fall for months. Thus, an additional 'quality category' was set up. QC 2 had to have data from at least four years covering not < 16 months, because below this threshold the use of RMA regression frequently resulted in insignificant relationships (see Sect. 2.3.2).
- The stations not meeting any of the criteria above (QC 3) were excluded from the analysis.

The possibility was entertained that stations situated close to each other (within 10 km) could be merged to improve the input data for LMWL estimation. Since certain monitoring sites had been relocated within a short distance, or restarted at a nearby locality after a multi-annual halt in monitoring, the datasets for such nearby stations were merged (Table S1). The coordinates of the one functioning longest from among those merged was used in the final dataset. In all cases the inter-station distance of the stations forming these merged datasets was smaller than 8 km. The final quality-controlled dataset contained 42 QC1 and 20 QC2 stations, of which 11 had been merged.

2.3.2. Reduced major axis (RMA) regression

Traditionally the LMWLs are defined employing ordinary least squares regression (OLS) or reduced major axis (RMA) regressions (IAEA, 1992). The conceptual difference between the two approaches is that while OLS regression minimizes the sum of the squared deviations of the predicted values, RMA minimizes both the vertical and the horizontal distances between each point and the regression line, i.e. it uses diagonal residuals that have slopes opposite to the slope of the regression line (Clarke, 1980). Since RMA is less prone to outliers, and more importantly, the relationship of the two assessed variables can be described by physical laws (Carroll and Ruppert, 1996), the application of RMA is more appropriate to the definition of the LMWL (Crawford et al., 2014; Putman et al., 2019).

A more advanced option could have been to use precipitation weighted RMA (PWRMA) regression (Crawford et al., 2014), but that would require precipitation amounts recorded for all δ_p values, a requirement not met in the present case. Moreover, studies support that the difference between slope and intercept values estimated by RMA and PWRMA agree within error bounds (Boschetti et al., 2019; Krajcar Bronić et al., 2020a). Therefore, in the present study RMA regression was applied to raw monthly δ_p values using the `lmodel2` package (Legendre, 2018) in `R` (R Core Team, 2019) with 2,000 permutations to obtain the significance values.

2.3.3. Interpolation techniques

Three major types of interpolation techniques were employed in the study, with different sets of predictors to obtain a spatially continuous map of the intercept and slope of the RMA regression. Inverse distance weighting (IDW), a traditional interpolation method (Webster and Oliver, 2008), and two machine learning (ML) methods, specifically random forest (RF) (Li et al., 2011; Liu et al., 2012) and support vector machine (SVM) (Cortes and Vapnik, 1995), were used.

IDW interpolation is a method in which each point of estimation is calculated as the average of nearby sample values, weighted by their distance from the estimation point. It does not make assumptions about spatial relationships, except for the basic assumption that nearby points are expected to be more closely related to the value at the estimation location than distant points. Two alternatives were trialed, linear (weighting power $\alpha = 1$; IDW_{p1}) and nonlinear (weighting power $\alpha = 2$; IDW_{p2}).

RF is a machine learning algorithm. In the procedure, a combination of a series of tree structure predictors is assessed. Here, each tree depends on the values of a random vector sampled independently with the same distribution for all trees in the forest. The generalization error for forests converges to a limit as the number of trees in the forest increases. The generalization error of a forest of tree classifiers depends on the strength of the individual trees in the forest and the correlation between them (Breiman, 2001). Its predictions are based on the average results of the decision trees, which use bootstrap sample (bagging) to eliminate the possibility of over-fitting; for details see e.g. Biau and Scornet (2016); Breiman (2001); Prasad et al. (2006). As with RF, SVM is another frequently used supervised machine learning technique for classification and regression purposes. However, the theory behind SVM is different to that of RF. It relies on the application of Kernel functions, which also means that SVM is a nonparametric technique, in finding a function that deviates from an observation by a value not greater than a given threshold value for each observation and at the same time is as flat as possible. As a consequence, the function fitted by SVM is the hyperplane that has the maximum number of observations (Cortes and Vapnik, 1995).

Six combinations of predictors which can influence the stable isotopic composition of precipitation, consequently the slope and intercept of the LWMLs in the region, were considered in the case of the ML algorithms:

- latitude, longitude (in Web Mercator EPSG: 3857), Köppen-Geiger climate class codes (category variable) with the approaches denoted as RF_{KG} & SVM_{KG},
- latitude, longitude and elevation (ele), denoted as RF_{ele} & SVM_{ele}, elevation was incorporated since the local orographic features may significantly change the isotopic composition of precipitation in the Mediterranean (Liotta et al., 2006; Liotta et al., 2013),
- latitude, longitude, Köppen-Geiger climate class codes, and elevation, denoted as $RF_{KG\text{-}ele}$ & $SVM_{KG\text{-}ele}$,
- the distance matrix of the monitoring stations, and again the Köppen-Geiger codes following the RFsp procedure of Hengl et al. (2004), with the approaches denoted as $RF_{sp\text{-}KG}$ and $SVM_{sp\text{-}KG}$,
- the distance matrix of the monitoring stations, and elevation, denoted as $RF_{sp\text{-}ele}$ and $SVM_{sp\text{-}ele}$,
- the distance matrix of the monitoring stations, the Köppen-Geiger climate class codes and elevation, denoted as $RF_{sp\text{-}KG\text{-}ele}$ and $SVM_{sp\text{-}KG\text{-}ele}$.

The IDW interpolation was performed using Golden Software Surfer 15 and GS+ 10. In the RF approach, the value of the `nodesize` and `mtry` parameters was selected automatically using the `tune` command of the `randomForestSRC` package (Ishwaran et al., 2021; Ishwaran et al., 2008) in `R` (R Core Team, 2019), while for RF_{sp}, these were chosen as 5 and 10 for the slope and intercept parameters, respectively, using the `ranger` package (Wright and Ziegler, 2015). The SVM modelling was carried out using the `caret` (Kuhn et al., 2020) and `e1071` (Meyer et al., 2019) `R` packages.

2.3.4. Validation

The results of the different interpolation schemes were validated by forming two pairs of training and validation datasets. Validation stations were only selected from those countries where there was more than one station available (not considering merged stations). The Validation-set 1 (Vs1; $n = 10$) consisted of one randomly chosen station from each country, preferably from its Q2 station(s). Validation-set 2 (Vs2; $n = 10$) consisted of the first stations in alphabetical order from each country (Table S1). The reason the stations were chosen from different countries was to avoid biased validation results that might arise due to some spatial clustering.

The sets of stations used in the actual interpolation were complementary to Vs1 and Vs2, and were referred to as Set 1 and Set 2, respectively. After applying the interpolation methods to estimate the slope and intercept of Set 1 and Set 2, the squared point-differences for stations in Vs1 and Vs2 were calculated. The performance of the 14 interpolation schemes was primarily evaluated using the squared errors of Vs1 and Vs2, while visual inspection of the interpolated maps was employed to check for systematic interpolation errors, artefacts etc. First and foremost, the median of the squared errors was taken into consideration rather than the mean, since latter is much more sensitive to outliers (Wilcox, 2003), which is a crucial strength in the case of a relatively small sample size, as with the present one.

3. Results and discussion

3.1. Local meteoric water lines in modern precipitation across the Mediterranean

In the estimations presented here, the point values of the stations and the pattern seen on the interpolated maps are compared with previous studies of the region. The slope of the $\delta^2H - \delta^{18}O$ relationship varied between ~5.9 and 8.3. The lowest values, some even falling below 7, were observed in the east and in the western parts and N Africa. The highest values, exceeding 8, in the north, in the Alpine foothills of Italy (Fig. 2A).

Considering subtropical arid or seasonally hot and dry regions (Köppen-Geiger climate class B and Cs), ~40% of the slopes obtained fall within the typical range (5 to 7) reported for these climate regions in a global assessment (Putman et al., 2019). The rest of the stations assigned to these climate classes had slightly steeper slopes (max Lake Massaciuccioli: 7.9 in zone Csa), which is still not unusual in these climates. Considering humid temperate and seasonally snow dominated regions (Köppen-Geiger climate class Cf and D), 77% of the obtained slopes fall within the typical range (7 to 8) for these climate regions reported in a global assessment (Putman et al., 2019). The remainder is in the vicinity of the southern Alps, where, as previously mentioned, the highest slope values are observed. In the subtropical arid or seasonally hot and dry regions (Köppen-Geiger climate classes B and Cs), almost all (90%) of the intercept values fall within the typical range (0 to 15‰) reported for these climate regions in (Putman et al., 2019). The outliers comprise mainly stations with low intercepts in central Iberia. In the case of humid temperate and seasonally snow dominated regions (Köppen-Geiger climate classes Cf and D), only 14% of the intercept values obtained fall within a typical range (−20 to 5‰) (Putman et al., 2019). This discrepancy may be due to the differing extent of various colder climate zones incorporated into the studies. It should be noted that the stations studied here are characteristically rather humid, and experience less snowfall (Fig. 1 and Table S1), whereas snowfall tends to result in negative intercepts (Putman et al., 2019).

The large-scale spatial patterns fit well into the estimations made for a continental transect across Europe, where slopes ranged from 6 to 10 (Lécuyer et al., 2020). In fact, from the western margin of the area studied up to the Adriatic (~12°E), a similar longitudinal trend is observed as that reported across the temperate and boreal regions of Europe, reaching a slope of 8 Lécuyer et al. (2020): Fig. 4 therein. Further eastward, however, while the slope of the relationship assessed from the continental transect continues to increase up to 9 (Lécuyer et al., 2020), in the case of the Mediterranean, it declines.

The spatial pattern of the intercept, on the other hand, shows a more complex pattern. In central Iberia, the intercept is < 3.5‰, while the coastal parts have values ranging between 2.7 and 6‰. Then, after a gradual increase, higher values are seen surrounding the Adriatic Sea, peaking at > 10‰ in northeastern Italy and Slovenia (Fig. 2B), matching the area of the steepest slopes (Fig. 2A). Eastward from the Adriatic, a gradual decrease is observed. Around 17°E intercepts of 7.5‰ are observed to decrease to around 5‰ (20–23°E). A subregional pattern is seen surrounding the Black Sea, where intercept values are < 3.2‰ (Fig. 1A). It is a common climatic feature of the 'low-intercept' areas (both central Iberia and this particular region) that the summer is characterized by very dry conditions (Table S1). An explicit contrast is observed in the southeastern sector of the Mediterranean Basin, where

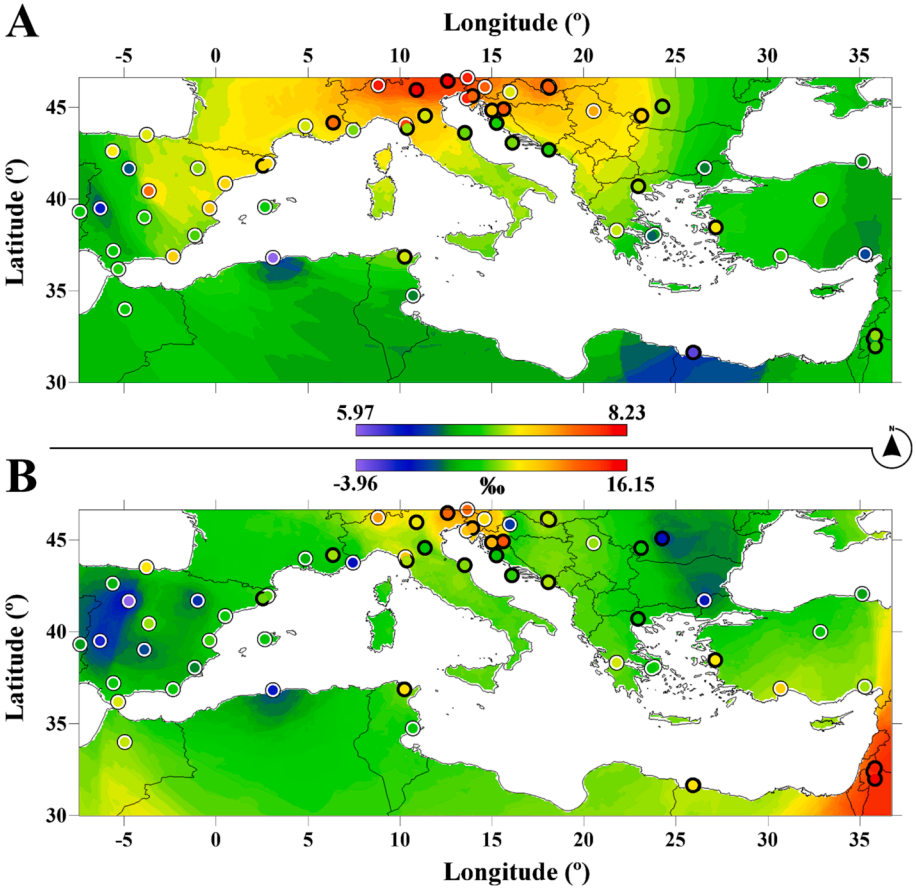

Fig. 2. Slope (A) and intercept (B) of the $RF_{sp\text{-}ele}$ interpolated map of the Mediterranean LWMLs. The colored circles with a white outline indicate the LMWLs of the precipitation monitoring stations belonging to QC1, while tha black outline denotes QC2 stations. The GeoTIFF versions of the maps can be found as Figs. S1 and S2 for the slope and the intercept, respectively.

altogether the highest (> 16‰) intercept values are to be found (Fig. 2B).

In the northern part of Africa, the number of stations used to estimate the LMWLs and interpolate those is smaller and much less continuous compared to the other regions in the Mediterranean (Fig. 2). Therefore, attention should be paid to these points when the estimations for this specific sub-region are used.

3.2. Performance evaluation of the spatially continuous estimations of the LMWLs across the Mediterranean region

In choosing the best performing interpolation method, the median, the upper quartile and the interquartile interval obtained squared differences and the question of how prone the method was to showing extreme outliers were all considered. If the number of squared differences classified as extreme outliers (Fig. 3) is ≥10% (practically $n = 2$) for either the slope or the intercept, said method is discarded. This was true for all the SVM approaches regardless of the predictors applied. Since the SVM methods gave the most extreme outliers in the case of the slope and intercept, those were not considered in the following. It was also determined that there was no significant difference either between the medians as calculated using Mood's independent samples median test (Mood, 1950) (asymptotic significance $p = .549$ and .72 for the slope and intercept, respectively), or in the distribution of the squared errors between the three models with the best performance based on independent samples using the Kruskal-Wallis test (Kruskal and Wallis, 1952), which yielded values of $H(2) = .663, p = .718$ for the slope and $H(2) = .82, p = .644$.

The inverse distance approaches performed worst in the case of the slope regarding the median and the upper quartile (Fig. 3A) and regarding the median in the case of the intercept (Fig. 3B). Therefore, the RF approaches with the different combination of predictors seemed the most promising. $RF_{sp\text{-}ele}$ was the only combination that gave the most promising results for the slope and intercept as well. This was not true for the other options, because those gave incoherent errors: for some the squared errors were higher for the slope while indicating relatively smaller errors for the intercept, and vice-versa (Fig. 3). Thus, to be consistent, the random forest approach with buffer distance, and with the inclusion of elevation as predictors ($RF_{sp\text{-}ele}$) was chosen to provide the best interpolation for the slope (Fig. 2A) and the intercept (Fig. 2B) of the Mediterranean LWML.

3.3. Spatial patterns and regional differences

Comparing not only the estimated point values (Sect. 3.2) but the spatial trend seen in the spatially continuous interpolated products

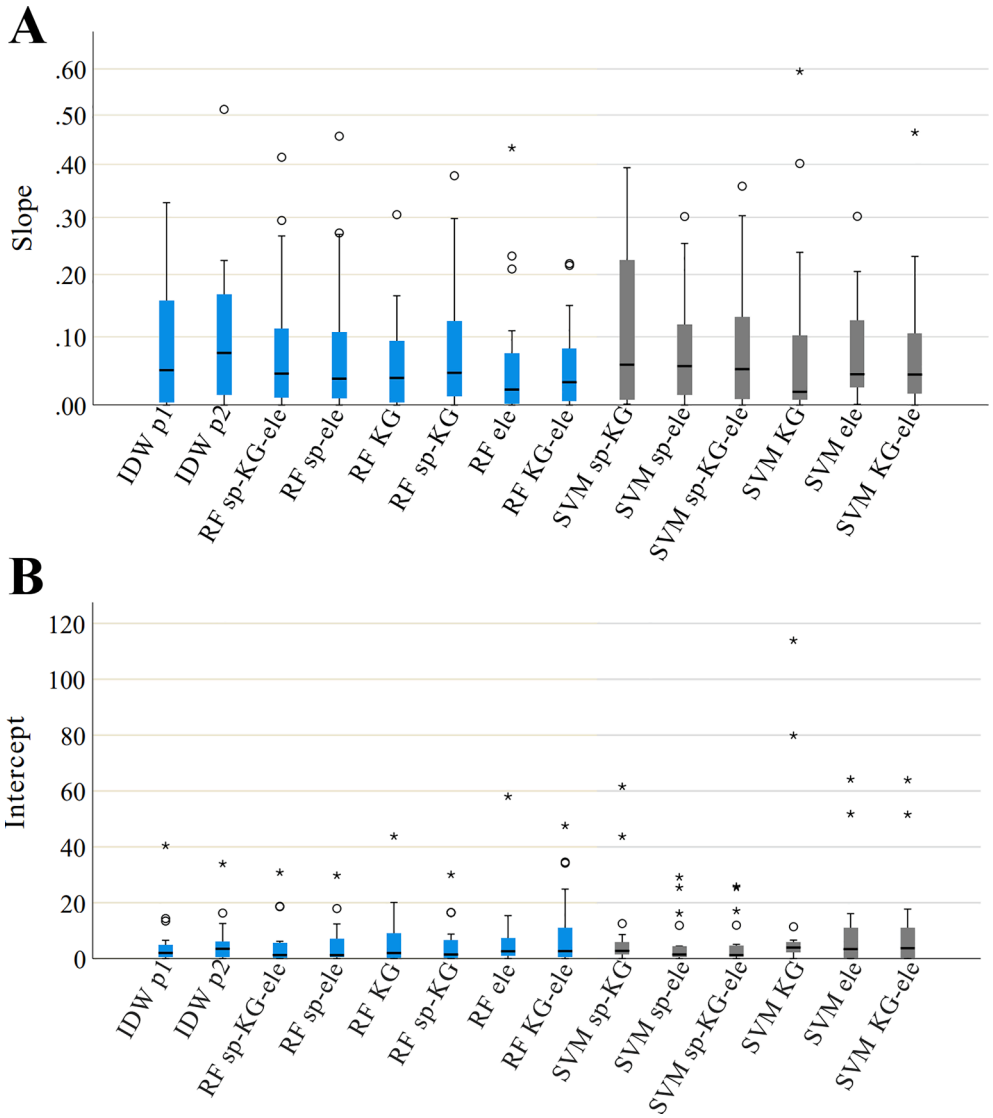

Fig. 3. Box-and-whiskers plots of the squared errors. Boxes represent the squared errors between the measured values of both sets of validation stations (Vs1 and Vs2) and the values for slope A) and the intercept B) estimated at their locations. The boxes indicate the interquartile interval, the black line in the middle the median, while the values outside 1.5-times the interquartile interval are indicated by a circle and the ones with higher values than 3 times the interquartile range are extreme values indicated with an asterisk (Kovács et al., 2012). Grey bars represent the errors of the SVM results omitted in the first round of the analysis, see text for details.

(Fig. 2 and Figs. S1 and S2), it was observed that these concur with the findings documented in numerous studies from the region over the decades. There are, however, some differences that are explained later in this section.

A recent regional study described the LMWL across NW Iberia on the basis of a small regional monitoring network (Moreno et al., 2021) partially overlapping with the chosen timeframe (2010–2012), but not meeting the quality criteria described in Sect. 2.3.1. Apart from Barcelona and Mallorca, the stations used in that study were not included in the present analysis, hence offering the possibility of an independent comparison to assess the interpolated LMWL parameters. Along the Cantabrian Coast, the difference in the slope between the presented model and a reference study (Moreno et al., 2021) is 0.6. This may be because the region is on the border of the present study area, where the slope values were merely extrapolated. In contrast to this, the slope does represent quite a good match with the other stations (Moreno et al., 2021), with an average difference of 0.12. In an Iberian regional reference study, the intercept ranges between 1 and 5‰ (Moreno et al., 2021), which is similar to the values in the present estimations (Fig. 2. B).

Heading east, the regional trend previously documented across the Apennine Peninsula (Giustini et al., 2016) is in harmony with the pattern documented here: a continuous decrease in slope (from 8 to 7) and intercept (from 9.5 to 6‰) from north to south (Fig. 2A). Specifically, the slope parameter displays a good match over the whole region (Fig. 2A), while the values of the intercept are smaller (Fig. 2B) compared to those in a reference study (Giustini et al., 2016). If the present estimations are compared with the LMWL of a more localized study from NE Italy (Masiol et al., 2021), the slope values show a good match, while the intercept estimated in the present work is slightly higher by ~1‰. On the SE coast of the Gulf of Genoa (Fig. 1A), a regional study estimated a slope of 7.28 and intercept: 7.3‰ (Natali et al., 2021), which gave a rather good match with the presented modelled values (Fig. 2). It should be noted, however, that two out of the four central Italian stations were used in the interpolation exercise after preprocessing. Therefore, this comparison cannot be taken as fully independent. Similar slope and intercept values are observed across Sicily compared to the sub-regional outcrop of the model for the Apennine Peninsula (Giustini et al., 2016), and a better match is seen in the highly elevated NW coastal stations of Sicily when compared to a sub-regional model of the island (Liotta et al., 2006). Compared to a study assessing the regional LMWLs in Sicily, the presented slope values are slightly higher and so are the intercept values (~1‰) (Liotta et al., 2013), although this difference might come from the relatively short period covered (Jul 2004 – Jun 2006), which does not meet the necessary "four year criterion" (Putman et al., 2019).

An independent dataset from eastern Serbia incorporating three stations overlaps with the study period (Vasić, 2017). The specific locations of the stations used in that reference work were not documented and the temporal coverage was not continuous, thus these could only be used with reservations for comparison and are not included in the modeling. The slope of individual stations ($n = 3$) ranged from 6.6 to 7.2, with the intercept spanning −2.4 to 4.8‰ (Vasić, 2017). The present model provided a spatially much smoother and somewhat higher estimation for the slope and intercept for the corresponding area, with values of ~7.4 and ~5.3‰, respectively (Fig. 2), probably due to their applied method (OLS) and temporal gaps and in the reference data (Vasić, 2017).

Considering the southern sector of the Balkan Peninsula, reported LMWLs display an unusually large scattering in slope and intercept (from 5.5 to 9.2 and from −1.2 to 21‰, respectively), even for locations close to each other in southern Greece (Dotsika et al., 2010). On the contrary, the macro-regional Mediterranean model presented here displays much smoother, and hence realistic, estimates of the LMWL parameters. Heading further east, the slope and intercept indicate a rather meridional trend across Greece. The slope gradually decreases from ~7.3 to ~6.9 going west to east across Greece (Fig. 2A), while the intercept decreases from the Albanian-Greek border (~5.9‰) to < 3‰ also towards Turkey (Fig. 2B).

For the final subregional comparison, in Cyprus, a LMWL ($\delta^2H = 6.58 \pm 0.13 \times \delta^{18}O + 12.64 \pm 0.91$) was derived in a recent study from the mean precipitation-weighted values of 16 monitoring stations (Christofi et al., 2020), updating older findings based on many fewer stations, $\delta^2H = 5.75 \times \delta^{18}O + 3.6$ (Jacovides, 1979). Taking the previous estimations into account, the present model's slope for the area (~6.8) agrees well with the most recent one, while the intercept (~7‰) is below the recent estimate, but definitely higher than the older study's intercept value.

Regarding North Africa, a study combining rainfall events and monthly data from 17 monitoring stations defined two LMWLs (Ait Brahim et al. (2016): Fig. 5 therein), the estimated parameters of which are both higher than those yielded by the present estimation (slope ~7; intercept ~7.5‰). This may well be due to relative scarcity of station data in this subregion passing the quality control requirements (Sect. 2.3.1) of the present study.

3.4. Regional meteoric water lines in the eastern and western Mediterranean domain?

In the eastern sector of the region the current macro-regional Mediterranean model (i) displays a slightly higher slope (around and between 6.8 and 6.9) compared to previous regional works for precipitation from the 1960s (< 6.3; (Gat and Dansgaard, 1972)), but (ii) better agrees if all rain events from the 1990s are considered (slope < 8; (Ayalon et al., 1998)). The present model's highest intercept values scatter around 15‰ in the Eastern Mediterranean sector. Thus, neither the slope, nor the intercept reproduce the frequently cited benchmark values of the $\delta^2H = 8 \times \delta^{18}O + 22$ EMMWL 'variant'. It should be noted that both parameters show a quite homogeneous pattern in this subregion, supporting the derivation of a regional MWL. The EMMWL may well have proven itself to be a useful isotope-hydrological benchmark, but cannot be taken as an actual empirical relationship validly describing the meteoric waters in the eastern Mediterranean following the fundamental rules of deriving meteoric water line(s) (Gat, 2005).

In the western Mediterranean the presence of a regional MWL has been suggested, with a slope of 8 and intercept 13.7‰ (Celle-Jeanton et al., 2001) overarching a vast part of the area. However, the present model – based on a much higher number of stations – shows clear differences across the domain under consideration (Fig. 2). The slope varies between ~6.5 and ~7.5, with the lowest values in Algeria, and the highest in Iberia (Fig. 2A), while the intercept ranges from ~2.5 to ~6.5‰, with the lowest values seen again in Algeria, and the highest values near the Gulf of Genoa (Fig. 2B). The spatial heterogeneity of LMWL parameters based on precipitation from between 2000 and 2015 in the western Mediterranean Basin does not support the definition of a uniform regional MWL for this region. Further use of the "Western Mediterranean Meteoric Water Line" as an isotope hydrological benchmark therefore seems to be untenable. Instead, the use of (i) the local estimates from nearby stations with long-term monitoring, or in the absence of a nearby station, (ii) estimates retrieved from the current interpolated product is recommended (Fig. 2).

4. Conclusions

In the study the long-term precipitation stable isotopic data of 249 Mediterranean precipitation monitoring stations were assessed to derive a revised and extended spatially continuous geostatistical model of the local meteoric water lines of the region for the early twenty-first century. In the chosen focus period (2000–2015) rigorous preprocessing consisted of iteratively assessing (i) the local indicator of spatial association together with (ii) d-excess values to find outliers. As a result, 62 stations were retained with at least four years of data coverage ensuring a quality-controlled dataset for the derivation of the LMWLs with RMA

regression and the interpolation of the slope and intercept of the δ^2H – $\delta^{18}O$ relationship across the region using random forest interpolation with buffer distance. The slope and intercept of the LMWLs ranged from ~5.9 to 8.2 and −3.9 to 16.1‰, respectively.

The macro-regional Mediterranean model of δ^2H – $\delta^{18}O$ covariance presented here provides spatially continuous predictions of the slope and intercept of the LMWL of modern (post-2000 CE) precipitation, updating the results of subregional studies from the twentieth century. The model provides an opportunity to revisit the classical concepts of the EMMWL and the WMMWL. With regard to the former, the coherent pattern of rather high intercept values in the eastern Mediterranean reinforces the validity and utility of the concept of the EMMWL for the 21st century, too, but in the west there was no homogeneous pattern of LMWL parameters. On the basis of the results of the present model, it is therefore suggested that the WMMWL should be abandoned as an isotope-hydrological benchmark for modern precipitation. The sub-regional to regional differences observed in the interpolated LMWLs highlight the importance of deriving fine scale spatially continuous estimations of the MWL and not aggregating data together from numerous stations that may be hundreds or even thousands of kilometers apart. It is therefore advised that either local estimates from close stations with long-term monitoring, or in the absence of a nearby station, estimates retrieved from the current interpolated product (Figs. S1 and S2) should be used for the region.

Author contributions

Z.K conceived and designed the study with contribution from I.G.H. I.G.H, D.E, A.E.S., and G.Sz performed the analysis. D.E. and I.G.H produced the figures. I.G.H and Z.K wrote the paper, with contributions from D.E., A.E.S., G.Sz. and P.V. The FLAE approach was applied to the sequence of authors; see https://doi.org/10.1371/journal.pbio.0050018. All authors have read and agreed to the published version of the manuscript.

Funding

This research was supported by the National Research, Development and Innovation Office under Grants SNN118205 and by the Slovenian Research Agency ARRS under Grants N1-0054 and P1-0143.

Data availability statement

Publicly available datasets were analyzed in this study. This data can be found at: https://nucleus.iaea.org/wiser/index.aspx and in the papers cited, see Table S1 and Sect. 2.2 for further details.

Declaration of Competing Interest

The authors declare that they have no known competing financial interests or personal relationships that could have appeared to influence the work reported in this paper.

Data availability

The source of the used data is explained in the Data Availability Statement in the MS.

Acknowledgments

The authors thank Paul Thatcher for his work on the English version; the authors are grateful for Christof Christofi, Jasper Wassenburg, Enrico Selmo and Roxana Ionete for providing data. The results of this study have been discussed within the COST Action: “WATSON” CA19120.

Appendix A. Supplementary data

Supplementary data to this article can be found online at https://doi.org/10.1016/j.jhydrol.2022.128925.

References

Aggarwal, P.K., Gat, J.R., Froehlich, K.F.O., 2005. Isotopes in the Water Cycle: Past. Present and Future of a Developing Science, Springer, Netherlands, Dordrecht, p. 382.

Ait Brahim, Y., et al., 2016. Elucidating the climate and topographic controls on stable isotope composition of meteoric waters in Morocco, using station-based and spatially-interpolated data. J. Hydrol. 543, 305–315. https://doi.org/10.1016/j.jhydrol.2016.10.001.

Anselin, L., 1996. The Moran scatterplot as an ESDA tool to assess local instability in spatial association. In: Fischer, M., Scholten, H.J., Unwin, D. (Eds.), Spatial Analytical Perspectives on GIS Routledge, London, UK, pp. 111-126.

Argiriou, A.A., Lykoudis, S., 2006. Isotopic composition of precipitation in Greece. J. Hydrol. 327 (3), 486–495. https://doi.org/10.1016/j.jhydrol.2005.11.053.

Ayalon, A., Bar-Matthews, M., Sass, E., 1998. Rainfall-recharge relationships within a karstic terrain in the Eastern Mediterranean semi-arid region, Israel: $\delta^{18}O$ and δD characteristics. J. Hydrol. 207 (1), 18–31. https://doi.org/10.1016/S0022-1694(98)00119-X.

Bajjali, W., Abu-Jaber, N., 2001. Climatological signals of the paleogroundwater in Jordan. J. Hydrol. 243 (1), 133–147. https://doi.org/10.1016/S0022-1694(00)00409-1.

Bartholy, J., Pongrácz, R., Pattantyús-Ábrahám, M., 2009. Analyzing the genesis, intensity, and tracks of western Mediterranean cyclones. Theor. Appl. Climatol. 96 (1), 133–144. https://doi.org/10.1007/s00704-008-0082-9.

Biau, G., Scornet, E., 2016. A random forest guided tour. TEST 25 (2), 197–227. https://doi.org/10.1007/s11749-016-0481-7.

Bojar, A.-V., Halas, S., Bojar, H.-P., Chmiel, S., 2017. Stable isotope hydrology of precipitation and groundwater of a region with high continentality, South Carpathians, Romania. Carpathian J. Earth Environ. Sci. 12 (2), 513–524.

Boschetti, T., Cifuentes, J., Iacumin, P., Selmo, E., 2019. Local meteoric water line of Northern Chile (18° S–30° S): an application of error-in-variables regression to the oxygen and hydrogen stable isotope ratio of precipitation. Water 11 (4), 791.

Bottyán, E., Czuppon, G., Weidinger, T., Haszpra, L., Kármán, K., 2017. Moisture source diagnostics and isotope characteristics for precipitation in east Hungary: implications for their relationship. Hydrol. Sci. J. 62 (12), 2049–2060. https://doi.org/10.1080/02626667.2017.1358450.

Boumaiza, L., Chesnaux, R., Drias, T., Walter, J., Stumpp, C., 2021. Using vadose-zone water stable isotope profiles for assessing groundwater recharge under different climatic conditions. Hydrol. Sci. J. 66 (10), 1597–1609. https://doi.org/10.1080/02626667.2021.1957479.

Bowen, G.J., 2008. Spatial analysis of the intra-annual variation of precipitation isotope ratios and its climatological corollaries. J. Geophys. Res. Atmos. 113 (D5) https://doi.org/10.1029/2007JD009295.

Bowen, G.J., Cai, Z., Fiorella, R.P., Putman, A.L., 2019. Isotopes in the water cycle: regional- to global-scale patterns and applications. Annu. Rev. Earth Planet. Sci. 47 (1), 453–479. https://doi.org/10.1146/annurev-earth-053018-060220.

Breiman, L., 2001. Random forests. Mach. Learn. 45 (1), 5–32. https://doi.org/10.1023/A:1010933404324.

Brkić, Ž., Kuhta, M., Hunjak, T., Larva, O., 2020. Regional isotopic signatures of groundwater in Croatia. Water 12 (7), 1983.

Carroll, R.J., Ruppert, D., 1996. The use and misuse of orthogonal regression in linear errors-in-variables models. Am. Statist. 50 (1), 1–6. https://doi.org/10.1080/00031305.1996.10473533.

Celle-Jeanton, H., Travi, Y., Blavoux, B., 2001. Isotopic typology of the precipitation in the Western Mediterranean Region at three different time scales. Geophys. Res. Lett. 28 (7), 1215–1218. https://doi.org/10.1029/2000GL012407.

Cervi, F., et al., 2017. Isotopic features of precipitation and groundwater from the Eastern Alps of Italy: results from the Mt. Tinisa hydrogeological system. Environ. Earth Sci. 76 (12), 410. https://doi.org/10.1007/s12665-017-6748-9.

Christofi, C., Bruggeman, A., Kuells, C., Constantinou, C., 2020. Isotope hydrology and hydrogeochemical modeling of Troodos Fractured Aquifer, Cyprus: The development of hydrogeological descriptions of observed water types. Appl. Geochem. 123, 104780 https://doi.org/10.1016/j.apgeochem.2020.104780.

Ciric, D., Nieto, R., Losada, L., Drumond, A., Gimeno, L., 2018. The mediterranean moisture contribution to climatological and extreme monthly continental precipitation. Water 10 (4).

Clark, I.D., Fritz, P., 1997. Environmental Isotopes in Hydrogeology. Taylor & Francis.

Clarke, M.R.B., 1980. The reduced major axis of a bivariate sample. Biometrika 67 (2), 441–446. https://doi.org/10.1093/biomet/67.2.441.

Cook, B.I., Anchukaitis, K.J., Touchan, R., Meko, D.M., Cook, E.R., 2016. Spatiotemporal drought variability in the Mediterranean over the last 900 years. J. Geophys. Res. Atmos. 121 (5), 2060–2074. https://doi.org/10.1002/2015JD023929.

Cortes, C., Vapnik, V., 1995. Support-vector networks. Mach. Learn. 20 (3), 273–297. https://doi.org/10.1007/BF00994018.

Craig, H., 1961. Isotopic variations in meteoric waters. Science 133 (3465), 1702–1703. https://doi.org/10.1126/science.133.3465.1702.

Crawford, J., Hughes, C.E., Lykoudis, S., 2014. Alternative least squares methods for determining the meteoric water line, demonstrated using GNIP data. J. Hydrol. 519, 2331–2340. https://doi.org/10.1016/j.jhydrol.2014.10.033.

Dansgaard, W., 1964. Stable isotopes in precipitation. Tellus 16, 436–468.
Dotsika, E., Lykoudis, S., Poutoukis, D., 2010. Spatial distribution of the isotopic composition of precipitation and spring water in Greece. Global Planet. Change 71 (3), 141–149. https://doi.org/10.1016/j.gloplacha.2009.10.007.
El Ouali, A., et al., 2022. Isotopic characterization of rainwater for the development of a local meteoric water line in an arid climate: the Case of the Wadi Ziz Watershed (South-Eastern Morocco). Water 14 (5), 779.
El-Asrag, A., 2005. Effect of synoptic and climatic situations on fractionation of stable isotopes in rainwater over Egypt and east Mediterranean. Isotopic composition of precipitation in the Mediterranean Basin in relation to air circulation patterns and climate 51–73.
Elghawi, R., Pekhazis, K., Doummar, J., 2021. Multi-regression analysis between stable isotope composition and hydrochemical parameters in karst springs to provide insights into groundwater origin and subsurface processes: regional application to Lebanon. Environ. Earth Sci. 80 (6), 230. https://doi.org/10.1007/s12665-021-09519-4.
Erdélyi, D., et al., 2023. Predicting spatial distribution of stable isotopes in precipitation by classical geostatistical- and machine learning methods. J. Hydrol., 129129 https://doi.org/10.1016/j.jhydrol.2023.129129.
Fernández-Chacón, F., Benavente, J., Rubio-Campos, J.C., Kohfahl, C., Jiménez, J., Meyer, H., Hubberten, H., Pekdeger, A., 2010. Isotopic composition ($\delta^{18}O$ and δD) of precipitation and groundwater in a semi-arid, mountainous area (Guadiana Menor basin, Southeast Spain). Hydrol. Process. 24 (10), 1343–1356. https://doi.org/10.1002/hyp.7597.
Fischer, M.J., Mattey, D., 2012. Climate variability and precipitation isotope relationships in the Mediterranean region. J. Geophys. Res. Atmos. 117 (D20) https://doi.org/10.1029/2012JD018010.
Fórizs, I., 2003. Isotopes as natural tracers in the watercycle: examples from the Carpathian Basin. Studia UBB Physica 1 (48), 69–77.
Fórizs, I., Kern, Z., Csicsák, J., Csurgó, G., 2020. Monthly data of stable isotopic composition ($\delta^{18}O$, $\delta^{2}H$) and tritium activity in precipitation from 2004 to 2017 in the Mecsek Hills, Hungary. Data in Brief 32, 106206. https://doi.org/10.1016/j.dib.2020.106206.
García-Ruiz, J.M., López-Moreno, J.I., Vicente-Serrano, S.M., Lasanta-Martínez, T., Beguería, S., 2011. Mediterranean water resources in a global change scenario. Earth Sci. Rev. 105 (3), 121–139. https://doi.org/10.1016/j.earscirev.2011.01.006.
Gat, J.R., 1996. Oxygen and hydrogen isotopes in the hydrologic cycle. Annu. Rev. Earth Planet. Sci. 24 (1), 225–262. https://doi.org/10.1146/annurev.earth.24.1.225.
Gat, J.R., 2005. Some Classical Concepts of Isotope Hydrology. In: Aggarwal, P.K., Gat, J. R., Froehlich, K.F.O. (Eds.), Isotopes in the Water Cycle: Past, Present and Future of a Developing Science. Springer Netherlands, Dordrecht, pp. 127-137. DOI:10.1007/1-4020-3023-1_10.
Gat, J.R., Carmi, I., 1970. Evolution of the isotopic composition of atmospheric waters in the Mediterranean Sea area. J. Geophys. Res. (1896–1977), 75(15): 3039-3048. Doi: https://doi.org/10.1029/JC075i015p03039.
Gat, J.R., Dansgaard, W., 1972. Stable isotope survey of the fresh water occurrences in Israel and the Northern Jordan Rift Valley. J. Hydrol. 16 (3), 177–211. https://doi.org/10.1016/0022-1694(72)90052-2.
Gat, J.R., Mook, W.G., Meijer, H.A., 2001. Environmental isotopes in the hydrological cycle, 2. International Atomic Energy Agency, Paris, 73 pp.
Giustini, F., Brilli, M., Patera, A., 2016. Mapping oxygen stable isotopes of precipitation in Italy. J. Hydrol.: Reg. Stud. 8, 162–181. https://doi.org/10.1016/j.ejrh.2016.04.001.
Golobočanin, D., Ogrinc, N., Bondzić, A., Miljević, N., 2007. Isotopic characteristics of meteoric waters in the Belgrade region. Isot. Environ. Health Stud. 43 (4), 355–367. https://doi.org/10.1080/10256010701702929.
Hatvani, I.G., Erdélyi, D., Vreča, P., Kern, Z., 2020. Analysis of the spatial distribution of stable oxygen and hydrogen isotopes in precipitation across the Iberian Peninsula. Water 12 (2), 481. https://doi.org/10.3390/w12020481.
Hengl, T., Heuvelink, G.B.M., Stein, A., 2004. A generic framework for spatial prediction of soil variables based on regression-kriging. Geoderma 120 (1), 75–93. https://doi.org/10.1016/j.geoderma.2003.08.018.
Hoerling, M., et al., 2012. On the increased frequency of Mediterranean drought. J. Clim. 25 (6), 2146–2161. https://doi.org/10.1175/jcli-d-11-00296.1.
Hssaisoune, M., et al., 2022. Isotopic and chemical tracing for residence time and recharge mechanisms of groundwater under semi-arid climate: case from Rif mountains (Northern Morocco). Geosciences 12 (2), 74.
Hunjak, T., Lutz, H.O., Roller-Lutz, Z., 2013. Stable isotope composition of the meteoric precipitation in Croatia. Isot. Environ. Health Stud. 49 (3), 336–345. https://doi.org/10.1080/10256016.2013.816697.
IAEA, 1992. Statistical treatment of data on environmental isotopes in precipitation. Technical Report Series International Atomic Energy Agency, Vienna, 781place pp.
IAEA, 2005. Isotopic composition of precipitation in the Mediterranean Basin in relation to air circulation patterns and climate. TECDOC Series. International Atomic Energy Agency, Vienna, Austria, 223 pp.
Iglesias, A., Garrote, L., Flores, F., Moneo, M., 2007. Challenges to manage the risk of water scarcity and climate change in the Mediterranean. Water Resour. Manag. 21 (5), 775–788. https://doi.org/10.1007/s11269-006-9111-6.
Ishwaran, H., Kogalur, U., Kogalur, M., 2021. RandomForestSRC: Fast Unified Random Forests for Survival. Regression, and Classification (RF-SRC) [(accessed on 16 July 2020)].
Ishwaran, H., Kogalur, U.B., Blackstone, E.H., Lauer, M.S., 2008. Random survival forests. Annals Appl. Stat., 2(3): 841-860, 20.
Jacovides, J., 1979. Environmental isotope survey (Cyprus). Final report on IAEA, research contract No: 1039, Ministry of Agriculture and Natural Resources, Department of Water Development, Nicosia, Cyprus.
Kattan, Z., 1997. Chemical and environmental isotope study of precipitation in Syria. J. Arid Environ. 35 (4), 601–615. https://doi.org/10.1006/jare.1996.0228.
Kelemen, F.D., Bartholy, J., Pongracz, R., 2015. Multivariable cyclone analysis in the Mediterranean region. Időjárás 119 (2), 159–184.
Kelley, C.P., Mohtadi, S., Cane, M.A., Seager, R., Kushnir, Y., 2015. Climate change in the Fertile Crescent and implications of the recent Syrian drought. Proc. Natl. Acad. Sci. 112 (11), 3241–3246. https://doi.org/10.1073/pnas.1421533112.
Kendall, C., Coplen, T.B., 2001. Distribution of oxygen-18 and deuterium in river waters across the United States. Hydrol. Process. 15 (7), 1363–1393. https://doi.org/10.1002/hyp.217.
Koeniger, P., Margane, A., 2014. Stable isotope investigations in the Jeita Spring catchment.
Koeniger, P., Margane, A., Abi-Rizk, J., Himmelsbach, T., 2017. Stable isotope-based mean catchment altitudes of springs in the Lebanon Mountains. Hydrol. Process. 31 (21), 3708–3718. https://doi.org/10.1002/hyp.11291.
Kottek, M.G., Jürgen; Beck, Christoph; Rudolf, Bruno; Rubel, Franz, 2006. World Map of the Köppen-Geiger climate classification updated. Meteorologische Zeitschrift, 15 (3): 259-263. DOI:10.1127/0941-2948/2006/0130.
Kovács, J. et al., 2012. Analysis of Water Quality Data for Scientists. In: Kostas Voudouris, Voutsa, D. (Eds.), Water Quality Monitoring and Assessment. InTech, pp. 65-94. DOI:10.5772/32173.
Krajcar Bronić, I., et al., 2020a. Long-term isotope records of precipitation in Zagreb, Croatia. Water 12 (1), 226.
Krajcar Bronić, I., et al., 2020b. Isotope Composition of precipitation, groundwater, and surface and lake waters from the Plitvice Lakes, Croatia. Water 12 (9), 2414.
Kruskal, W.H., Wallis, W.A., 1952. Use of ranks in one-criterion variance analysis. J. Am. Stat. Assoc. 47 (260), 583–621. https://doi.org/10.2307/2280779.
Kuhn, M. et al., 2020. caret: Classification and Regression Training. R package version 6.0-86. Astrophysics Source Code Library: Cambridge, MA, USA.
Lécuyer, C., Bojar, A.-V., Daux, V., Legendre, S., 2020. Geographic variations in the slope of the $\delta^{2}H$–$\delta^{18}O$ meteoric water line over Europe: a record of increasing continentality. Geological Society, London, Special Publications, 507: SP507-2020-68. DOI:10.1144/sp507-2020-68.
Legendre, P., 2018. lmodel2: Model II Regression. R package version 1.7-3.
Li, J., Heap, A.D., Potter, A., Daniell, J.J., 2011. Application of machine learning methods to spatial interpolation of environmental variables. Environ. Model. Softw. 26 (12), 1647–1659. https://doi.org/10.1016/j.envsoft.2011.07.004.
Liotta, M., et al., 2013. Isotopic composition of precipitation and groundwater in Sicily, Italy. Appl. Geochem. 34, 199–206. https://doi.org/10.1016/j.apgeochem.2013.03.012.
Liotta, M., Favara, R., Valenza, M., 2006. Isotopic composition of the precipitations in the central Mediterranean: origin marks and orographic precipitation effects. J. Geophys. Res. Atmos. 111 (D19) https://doi.org/10.1029/2005JD006818.
Liu, Y., Wang, Y., Zhang, J., 2012. New machine learning algorithm: random forest. In: Liu, B., Ma, M., Chang, J. (Eds.), Information Computing and Applications. Springer, Berlin Heidelberg, Berlin, Heidelberg, pp. 246–252.
Longinelli, A., et al., 2008. A stable isotope study of the Garda Lake, northern Italy: Its hydrological balance. J. Hydrol. 360 (1), 103–116. https://doi.org/10.1016/j.jhydrol.2008.07.020.
Longinelli, A., Anglesio, E., Flora, O., Iacumin, P., Selmo, E., 2006. Isotopic composition of precipitation in Northern Italy: reverse effect of anomalous climatic events. J. Hydrol. 329 (3), 471–476. https://doi.org/10.1016/j.jhydrol.2006.03.002.
Longinelli, A., Selmo, E., 2003. Isotopic composition of precipitation in Italy: a first overall map. J. Hydrol. 270 (1), 75–88. https://doi.org/10.1016/S0022-1694(02)00281-0.
Marchina, C., et al., 2020. Alternative methods to determine the $\delta^{2}H$-$\delta^{18}O$ relationship: An application to different water types. J. Hydrol. 587, 124951 https://doi.org/10.1016/j.jhydrol.2020.124951.
Marković, T., Karlović, I., Perčec Tadić, M., Larva, O., 2020. Application of stable water isotopes to improve conceptual model of alluvial aquifer in the Varaždin Area. Water 12 (2), 379.
Masiol, M., et al., 2021. Spatial distribution and interannual trends of $\delta^{18}O$, $\delta^{2}H$, and deuterium excess in precipitation across North-Eastern Italy. J. Hydrol. 598, 125749 https://doi.org/10.1016/j.jhydrol.2020.125749.
Meyer, D., Dimitriadou, E., Kurt, H., Andreas, W., Friedrich, L., 2019. e1071: misc functions of the department of statistics, probability theory group (Formerly: E1071), TU Wien. R package version 1. 7–1.
Mood, A.M., 1950. Introduction to the Theory of Statistics.
Moran, P.A.P., 1948. The interpretation of statistical maps. J. Roy. Stat. Soc.: Ser. B (Methodol.) 10 (2), 243–251.
Moreno, A., et al., 2021. Measurement report: Spatial variability of northern Iberian rainfall stable isotope values – investigating atmospheric controls on daily and monthly timescales. Atmos. Chem. Phys. 21 (13), 10159–10177. https://doi.org/10.5194/acp-21-10159-2021.
Natali, S., et al., 2021. Meteorological and geographical control on stable isotopic signature of precipitation in a western Mediterranean area (Tuscany, Italy): Disentangling a complex signal. J. Hydrol. 603, 126944 https://doi.org/10.1016/j.jhydrol.2021.126944.
Nelson, D.B., Basler, D., Kahmen, A., 2021. Precipitation isotope time series predictions from machine learning applied in Europe. Proc. Natl. Acad. Sci., 118(26): e2024107118. DOI:doi:10.1073/pnas.2024107118.
Paar, D., Mance, D., Stroj, A., Pavić, M., 2019. Northern Velebit (Croatia) karst hydrological system: results of a preliminary ^{2}H and ^{18}O stable isotope study. Geol. Croat. 72 (3), 205–213.

Paternoster, M., Liotta, M., Favara, R., 2008. Stable isotope ratios in meteoric recharge and groundwater at Mt. Vulture volcano, southern Italy. J. Hydrol. 348 (1), 87–97. https://doi.org/10.1016/j.jhydrol.2007.09.038.

Prasad, A.M., Iverson, L.R., Liaw, A., 2006. Newer classification and regression tree techniques: bagging and random forests for ecological prediction. Ecosystems 9 (2), 181–199. https://doi.org/10.1007/s10021-005-0054-1.

Putman, A.L., Fiorella, R.P., Bowen, G.J., Cai, Z., 2019. A global perspective on local meteoric water lines: meta-analytic insight into fundamental controls and practical constraints. Water Resour. Res. 55 (8), 6896–6910. https://doi.org/10.1029/2019WR025181.

R Core Team, 2019. R: A Language and Environment for Statistical Computing. R Foundation for Statistical Computing, Vienna, Austria.

Rindsberger, M., Jaffe, S., Rahamim, S., Gat, J.R., 1990. Patterns of the isotopic composition of precipitation in time and space: data from the Israeli storm water collection program. Tellus B 42 (3), 263–271. https://doi.org/10.1034/j.1600-0889.1990.t01-2-00005.x.

Rozanski, K., Araguás-Araguás, L., Gonfiantini, R., 1993. Isotopic patterns in modern global precipitation. In: Swart, P.K., Lohmann, K.C., Mckenzie, J., Savin, S. (Eds.), Climate Change in Continental Isotopic Records. American Geophysical Union, USA, pp. 1–36. https://doi.org/10.1029/GM078p0001.

Serianz, L., Cerar, S., Vreča, P., 2021. Using stable isotopes and major ions to identify recharge characteristics of the Alpine groundwater-flow dominated Triglavska Bistrica River. Geologija 64 (2), 205–220. https://doi.org/10.5474/geologija.2021.012.

Sharp, Z., 2017. Principles of stable isotope geochemistry.

Surić, M., Lončarić, R., Bočić, N., Lončar, N., Buzjak, N., 2018. Monitoring of selected caves as a prerequisite for the speleothem-based reconstruction of the Quaternary environment in Croatia. Quat. Int. 494, 263–274. https://doi.org/10.1016/j.quaint.2017.06.042.

Tappa, D.J., Kohn, M.J., McNamara, J.P., Benner, S.G., Flores, A.N., 2016. Isotopic composition of precipitation in a topographically steep, seasonally snow-dominated watershed and implications of variations from the global meteoric water line. Hydrol. Process. 30 (24), 4582–4592. https://doi.org/10.1002/hyp.10940.

Trabelsi, R., Matsumoto, T., Zouari, K., Trabelsi, M., Kumar, B., 2020. Investigation of paleoclimate signatures in Sfax deep groundwater (Southeastern Tunisia) using environmental isotopes and noble gases. Quat. Int. 547, 208–219. https://doi.org/10.1016/j.quaint.2019.04.001.

Túri, M., et al., 2019. Tracing groundwater recharge conditions based on environmental isotopes and noble gases, Lom depression, Bulgaria. J. Hydrol: Regional Stud. 24, 100611 https://doi.org/10.1016/j.ejrh.2019.100611.

Túri, M., et al., 2020. Paleotemperature reconstruction using environmental isotopes and noble gases in groundwater in Morocco. Hydrgeol. J. 28 (3), 973–986. https://doi.org/10.1007/s10040-020-02121-1.

Varlam, C., Duliu, O.G., Ionete, R.E., Costinel, D., 2021. Time series analysis of the δ^2H, $\delta^{18}O$ values in correlation with monthly temperature, relative humidity and precipitation in Râmnicu Vâlcea, Romania: 2012–2018. Geol. Soc. Lond. Spec. Publ. 507 (1), 77. https://doi.org/10.1144/SP507-2020-56.

Vasić, L.M., 2017. Geneza i uslovi cirkulacije voda kompleksnih karstnih sistema Kučajsko-beljaničkog masiva. University of Belgrade, Belgrade, Serbia, p. 409.

Vasić, L., Palcsu, L., Fen, H., 2019. Groundwater gravitational circulation of Karst Veliko Vrelo and Malo Vrelo springs by isotope and the noble gas method: case study of the Beljanica Massif. Environ. Earth Sci. 78 (10), 1–7.

Villani, L., Castelli, G., Piemontese, L., Penna, D., Bresci, E., 2022. Drought risk assessment in Mediterranean agricultural watersheds: A case study in Central Italy. Agric Water Manag 271, 107748. https://doi.org/10.1016/j.agwat.2022.107748.

Vreča, P., Bronić, I.K., Horvatinčić, N., Barešić, J., 2006. Isotopic characteristics of precipitation in Slovenia and Croatia: comparison of continental and maritime stations. J. Hydrol. 330 (3), 457–469. https://doi.org/10.1016/j.jhydrol.2006.04.005.

Vreča, P., Brenčič, M., Leis, A., 2007. Comparison of monthly and daily isotopic composition of precipitation in the coastal area of Slovenia. Isot. Environ. Health Stud. 43 (4), 307–321. https://doi.org/10.1080/10256010701702739.

Vreča, P., Krajcar Bronić, I., Leis, A., Brenčić, M., 2008. Isotopic composition of precipitation in Ljubljana (Slovenia). Geologija 51 (2), 169. https://doi.org/10.5474/geologija.2008.018.

Vreča, P., Krajcar Bronić, I., Leis, A., 2011. Isotopic composition of precipitation in Portorož (Slovenia). Geologija 54 (1), 129–137. https://doi.org/10.5474/geologija.2011.010.

Vreča, P., Krajcar Bronić, I., Leis, A., Demšar, M., 2014. Isotopic composition of precipitation at the Station Ljubljana (Reaktor), Slovenia – period 2007–2010. Geologija 57 (2), 217–230. https://doi.org/10.5474/geologija.2014.019.

Vreča, P., Bronić, I.K., Leis, A., 2015. Isotopic composition of precipitation at the station Portorož, Slovenia–period 2007–2010. Geologija 58 (2), 233–246. https://doi.org/10.5474/geologija.2015.019.

Vreča, P., Malenšek, N., 2016. Slovenian Network of Isotopes in Precipitation (SLONIP) – a review of activities in the period 1981–2015. Geologija 59 (1), 67–84. https://doi.org/10.5474/geologija.2016.004.

Vreča, P., Pavšek, A., Kocman, D., 2022. SLONIP-A slovenian web-based interactive research platform on water isotopes in precipitation. Water 14 (13), 2127. https://doi.org/10.3390/w14132127.

Wassenburg, J.A., et al., 2016. Reorganization of the North Atlantic Oscillation during early Holocene deglaciation. Nat. Geosci., advance online publication. https://doi.org/10.1038/ngeo2767.

Webster, R., Oliver, M.A., 2008. Geostatistics for Environmental Scientists. Geostatistics for Environmental Scientists. John Wiley & Sons Ltd 330 pp. https://doi.org/10.1002/9780470517277.index.

Wilcox, R.R., 2003. 3 - SUMMARIZING DATA. In: Wilcox, R.R. (Ed.), Applying Contemporary Statistical Techniques. Academic Press, Burlington, pp. 55-91. DOI: https://doi.org/10.1016/B978-012751541-0/50024-9.

Wright, M.N., Ziegler, A., 2015. ranger: A fast implementation of random forests for high dimensional data in C++ and R. arXiv preprint arXiv:1508.04409.

Yoshimura, K., 2015. Stable water isotopes in climatology, meteorology, and hydrology: A review. J. Meteorol. Soc. Japan. Ser. II 93 (5), 513–533. https://doi.org/10.2151/jmsj.2015-036.

Yüce, G., 2005. Determination of the recharge area and salinization degree of karst springs in the Lamas Basin (Turkey). Isot. Environ. Health Stud. 41 (4), 391–404. https://doi.org/10.1080/10256010500384747.